A new Kunitz-type snake toxin family associated with an original mode of interaction with the vasopressin 2 receptor

Laura Droctové, Justyna Ciolek, Christiane Mendre, Amélia Chorfa, Paola Huerta, Chrystelle Carvalho, Charlotte Gouin, Manon Lancien, Goran Stanajic-petrovic, Lorine Braco, et al.

A new Kunitz-type snake toxin family associated with an original mode of interaction with the vasopressin 2 receptor.

Laura Droctové[1], Justyna CioleK[1], Christiane Mendre[2], Amélia Chorfa[2], Paola Huerta[1], Chrystelle Carvalho[1], Charlotte Gouin[1], Manon Lancien[1], Guillaume Blanchet[1], Gregory Upert[1], Edwin De Pauw[3], Peggy Barbe[1], Mathilde Keck[1], Gilles Mourier[1], Bernard Mouillac[2], Denis Servent[1], Ricardo Rodriguez-de-la-vega[4], Loïc Quinton[3], and Nicolas Gilles[1]

[1]Commissariat a l'energie atomique et aux energies alternatives
[2]cnrs
[3]Liege University
[4]CNRS

July 3, 2021

Abstract

Background and purpose. Venomous animals express numerous Kunitz-type peptides. The mambaquaretin-1 (MQ1) recently identified from the Dendroaspis angusticeps venom is the most selective antagonist of the arginine-vasopressin V2 receptor (V2R) and the unique Kunitz-type peptide active on a GPCR. We aimed to exploit other mamba venoms to enlarge the V2R-Kunitz peptide family and get insight into the MQ1 molecular mode of action. Experimental approach. We used a bio-guided screening assay to identify novel MQs and placed them phylogenetically. Several newly identified MQs were produced by solid phase peptide synthesis. They were characterized in vitro by binding and functional tests andin vivo by diuresis measurement in rats. Key results. Eight additional MQs were identified with nanomolar affinities for the V2R, all antagonists. MQs form a new subgroup in the Kunitz family, close to the V2R non-active dendrotoxins and to 2 V2R active cobra toxins. Sequence comparison between active and non-active V2R Kunitz peptides highlighted 5 specific V2R positions. Four of them are involved in V2R activity and belong to the 2 large MQ1 loops. We finally determined that 8 positions, part of these 2 loops, interact with the V2R. The variant MQ1-K39A showed specificity for the human versus the rat V2R . Conclusions and implications. A third function and mode of action is now associated with the Kunitz-peptides. The number of MQ1 residues involved in V2R binding is large and may explain its absolute selectivity. MQ1-K39A represents the first step in the improvement of the MQ1 design for medicinal perspective.

A new Kunitz-type snake toxin family associated with an original mode of interaction with the vasopressin 2 receptor.

Laura Droctové[1], Justyna Ciolek[1], Christiane Mendre[2], Amélia Chorfa[2], Paola Huerta[1], Christelle Carvalo[1], Charlotte Gouin[1], Manon Lancien[1], Guillaume Blanchet[1], Gregory Upert[1], Edwin De Pauw[3], Peggy Barbe[1], Mathilde Keck[1], Gilles Mourier[1], Bernard Mouillac[2], Servent Denis[1], Ricardo C. Rodríguez de la Vega[4], Loïc Quinton[3], Nicolas Gilles[1*]

1 Université Paris Saclay, CEA, INRAE, Département Médicaments et Technologies pour la Santé (DMTS), SIMoS, 91191 Gif-sur-Yvette, France

2 Institut de Génomique Fonctionnelle, Université de Montpellier, CNRS, INSERM, 34094 Montpellier, France

3 Laboratory of Mass Spectrometry, MolSys Research Unit, University of Liège, Liège, Belgium

4 Ecologie, Systematique Evolution. CNRS, AgroParisTech, Université Paris-Saclay, 91400 Orsay, France

*to whom correspondence should be addressed:*nicolas.gilles@cea.fr*

Nicolas Gilles ORCID 0000-0001-6853-9764

Denis Servent ORCID 0000-0002-0774-1691

Authorship contribution statement

L.D, C.M., G.B., M.K., R.C.R.V., L.Q. and N.G. participated in research design.

L.D., J.C., C.M., A.C., P.H., C.C., C.G., M.L., G.B., G.U., P.B., M.K., G.M., R.C.R.V. and L.Q. conducted experiments.

L.D., G.B., G.M. and L.Q. contributed new reagents and analytic tools.

L.D., C.M., G.B., M.K., R.C.R.V. and N.G. performed the data analysis.

B.M., D.S., R.C.R.V., L.Q. and N.G. wrote or contributed to the writing of the manuscript.

Funding statement

This work was supported by the French Atomic and Alternative Energies.

Conflicts of interest statement

No conflict of interest

Data Availability Statement: No data have been shared.

Background and purpose. Venomous animals express numerous Kunitz-type peptides. The mambaquaretin-1 (MQ1) identified from the*Dendroaspis angusticeps* venom is the most selective antagonist of the arginine-vasopressin V2 receptor (V2R) and the unique Kunitz-type peptide active on a GPCR. We aimed to exploit other mamba venoms to enlarge the V2R-Kunitz peptide family and gain insight into the MQ1 molecular mode of action.

Experimental approach. We used a bio-guided screening assay to identify novel MQs and placed them phylogenetically. MQs were produced by solid phase peptide synthesis and characterized *in vitro* by binding and functional tests and *in vivo* by diuresis measurement in rats.

Key results. Eight additional MQs were identified with nanomolar affinities for the V2R, all antagonists. MQs form a new subgroup in the Kunitz family, close to the V2R non-active dendrotoxins and to 2 V2R active cobra toxins. Sequence comparison between active and non-active V2R Kunitz peptides highlighted 5 specific V2R positions. Four of them are involved in V2R activity and belong to the 2 large MQ1 loops. We finally determined that 8 positions, part of these 2 loops, interact with the V2R. The variant MQ1-K39A showed higher affinity for the hV2R but not for the rat V2R.

Conclusions and implications. A third function and mode of action is now associated with the Kunitz-peptides. The number of MQ1 residues involved in V2R binding is large and may explain its absolute selectivity. MQ1-K39A represents the first step in the improvement of the MQ1 design for medicinal perspective.

Abbreviations.

MQ Mambaquaretin

V2R arginine-vasopressin type 2 receptor

BPTI bovine pancreatic trypsin inhibitor

3FT 3 finger-fold toxins

Keywords: Snake venom, Kunitz peptide, V2R, antagonist, proteomics, peptide sequencing, peptide synthesis.

What is already known

The most selective V2R antagonist is a toxin extracted from the*Dendroaspis angusticeps* venom.

Other mamba species exist in Africa

Kunitz peptides are known to interact with their targets through small interaction surfaces.

What this study adds

The identification of a novel Kunitz family associated with a new pharmacological activity and a new mode of interaction.

What is the clinical significance

V2R is the unique validated therapeutic target for treating the autosomal dominant polycystic kidney disease, an unmet therapeutic need. MQ1 is a promising therapeutic agent against this disease. The MQ1/V2R interaction described here will help to improve MQ1 efficiency against this disease.

1. INTRODUCTION

Animal venoms are rich in biologically active molecules, named toxins, displaying a wide variety of biological properties, being enzymes (protease, phospholipases, nuclease, etc. . .), enzyme inhibitors (as serine protease inhibitor) or ligands for membrane proteins like ion channels or G protein-coupled receptors (GPCRs). In addition to their high affinity and selectivity for their various targets, animal toxins are also highly stable thanks to a reticulated and rigid structure. Mamba snake venoms are mostly composed of 2 toxins scaffolds, the 3 finger-fold toxins (3FT) and the Kunitz-type toxins (Ainsworth et al., 2017). 3FT are active on ionic channels like calcium channels, ASIC channels and nicotinic receptors, on aminergic GPCRs, as well as on enzymes and integrins receptors (Maïga et al., 2012; Blanchet et al., 2014; Kessler et al., 2017). The Kunitz-type toxins are homologous to the bovine pancreatic trypsin inhibitor (BPTI) and have been initially described as inhibitors of various serine and cysteine proteases (Kunitz and Northrop, 1936). In the early 1980s, mamba Kunitz-type toxins known as dendrotoxins were identified with neurotoxic effects driven by to their potassium channel blockade activities (Harvey, 2001). Later on, other Kunitz-type toxins were also described to inhibit calcium channels (Schweitz et al., 1994), vanilloid receptor 1 (Andreev et al., 2008) and ASIC channels (Bohlen et al., 2011). We recently assigned a new function to this structural family. The mambaquaretin-1 (MQ1) isolated from the green mamba snake venom is the most selective antagonist of the type 2 arginine-vasopressin (AVP) human receptor (hV2R) having a nanomolar affinity for the hV2R and no effect on 156 other GPCRs (Ciolek et al., 2017). Up to now, it is the sole Kunitz peptide known to be active on a GPCR. We furthermore validated MQ1 as a therapeutic solution to hyponatremia and polycystic kidney diseases and as a diagnostic agent to detect V2R *in vivo* (Ciolek et al., 2017, Droctové et al., 2020).

Kunitz peptides are made of 56 to 60 residues in length and are characterized by a highly conserved α/β/α conformation stabilized by three disulfide bridges (C1-C6/C2-C4/C3-C5). They also exhibit a strong intramolecular hydrophobic network (Huber et al., 1970). Their N-terminal extremity forms an alpha helix followed by a loop 1, which links to the first part of the antiparallel β sheet. The loop 2 connects the β sheet with the short C-terminal α helix. BPTI-like peptides interact with serine proteases *via* only 4 residues of its loop 1 and more particularly a dyad (residues 15 and 16) made of a basic residue followed by a glycine or alanine residue (Harper and Berger, 1967; Otlewski et al., 2001). Dendrotoxins, on the other hand, block the potassium channel Kv1.1 predominantly with its lysine and an aliphatic residue positioned in the N-terminal extremity of the peptides (Gasparini et al., 1998). These two pharmacophores are diametrically opposed in the Kunitz structure (Fig. 1), and are not present in MQ1. Consequently, MQ1 barely blocks Kv1.1 conductivity and inhibits trypsin activity at 25 μM concentrations only (Ciolek et al., 2017). When restoring the pharmacophore of the dendrotoxin in MQ1 (MQ1-S3K, numbering according to the MQ1 sequence),

potassium channel activity increases dramatically without affecting the V2R antagonism. When restoring the serine protease pharmacophore in MQ1 (MQ1-N15K+G16A), trypsin activity largely increases while the MQ1-V2R binding is disrupted (Ciolek et al., 2017).

In this study, we reassessed the diversity of mamba venoms by identifying 8 new mambaquaretins (MQs), which form a distinct functional monophyletic group among the Kunitz-type peptides.

These natural mambaquaretins altogether with synthetic variants brought new insights into MQ1 structure-activity relationships, highlighting the involvement of a large surface of the MQ1 structure in the V2R interaction, in sharp contrast to the way by which Kunitz-peptides block potassium channels or inhibit serine-proteases.

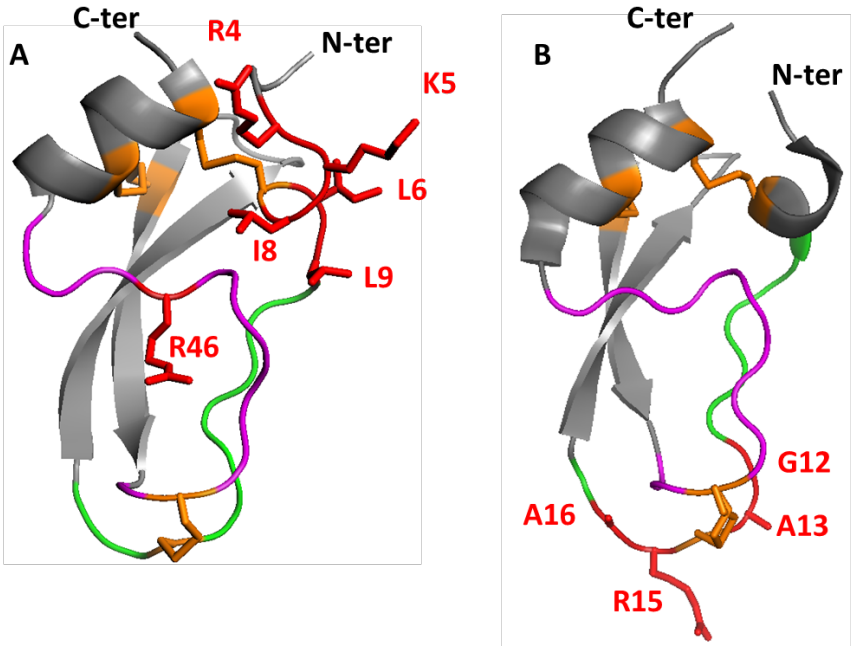

Figure 1. Pharmacophores of α-dendrotoxin and BPTI (in red sticks). Residues implicated in the binding of α-dendrotoxin (PDB: 1dtx) with Kv1.1 (Gasparini et al., 1998, **A**), and BPTI (P13A variant, PDB: 1qlq) with serine proteases (Otlewski et al., 2001, **B**). Loops are colored in green (loop 1) and magenta (loop 2).

2- METHODS

2.1 MQs identification . Venoms were fractionated as described (Ciolek et al., 2017). One gram of each Dendroaspis sp. venom (Latoxan, Valence, France) was separated into primary fractions by cation exchange liquid chromatography (5 x 40 cm) on the resin Source 15S using a multi-step NaCl gradient at 20 mL·min^{-1} on an Akta purifier (Pfizer, Quebec, Canada). The fractions were further purified by reverse-phase chromatography on a C18 Vydac preparative column (19.6 mm, 5 µm, 25 cm,), using a linear gradient from 0 to 100% acetonitrile in 0.1% trifluoroacetic acid in 100 min at a flow rate of 20 mL/min. Analytical high-pressure liquid chromatography (HPLC) was finally performed on a C18 Vydac column (4.6 mm, 5 mm, 15 cm) using a gradient of 0.5% acetonitrile per min and a flow rate of 1 mL/min. Protein concentrations were determined using the Bio-Rad protein assay with BSA as a standard. Toxin sequences were determined by mass analysis. Sequencing by in-source decay (ISD) MALDI-TOF was carried out with 15 µg of each fraction treated with 2 µL of 100 mM Tris(carboxyethyl)phosphine at 50°C and purified on a Zip-Tip C18 microcolumn. The matrix used for ISD experiments was 1,5-diaminonaphthalene (Accros). For peptide mass fingerprinting, 300 ng of purified toxins were reduced in 5 µL of 50 mM NH_4HCO_3, pH 8, by 2 µL of 250

mM DTT for 30 min at 56 °C, followed by 2.2 µL of 500 mM iodoacetamide for 1 h in the dark at room temperature. Mass analysis was made on a MALDI-TOF/TOF (rapifleX, Bruker Daltonics). Tandem mass spectrometry experiments were performed using LIFT-TOF/TOF technology. Data was acquired with Flex Control 3.0. Resulting spectra were analyzed with Biotools 3.2 and Sequence Editor 3.2 (Bruker Daltonics).

2.2 Binding assay with radioligand . ^{3}H-AVP was purchased from PerkinElmer (Courtaboeuf, France). Binding experiments on self-prepared CHO cells overexpressing vasopressin hV2R subtype or HEK cells transfected with a plasmid coding for the rat V2R, were performed as described (Ciolek et al., 2017; Droctové et al., 2020). Briefly, 1.5 nM ^{3}H-AVP in a 100 µL reaction mixture at room temperature in buffer composed of 50 mM Tris-HCl, pH 7.4, 10 mM $MgCl_2$, 1 g/L BSA was incubated with increasing concentrations of competitors for 3 hours. Non-specific binding was measured in the presence of 1 µM vasopressin. Incubation was stopped by filtration through 96 GF/C filter plates pre-incubated with 0.5% polyethylenimine. 25 µL of Microscint 0 were added onto each dry filter and the radioactivity was quantified on a TopCount beta counter with a 33% yield (PerkinElmer, Courtaboeuf, France). We fitted competition binding data with the one-site/state inhibition mass action curve using Kaleidagraph (Synergy software, Reading, USA). IC_{50} values were converted to K_i using 1 nM as Kd in the Cheng-Prusoff equation. Data represents independent experiments and are presented as the mean of $pK_i \pm$ SEM.

2.3 cAMP cell-based assay. The CHO cell line expressing hV2R was cultured at 37 °C in 5% CO_2 in DMEM containing 10% FCS and 100 units/ml penicillin/100 µg/ml streptomycin supplemented with 0.1 mM non-essential amino-acids and 0.4 mg/ml geneticin. We seeded CHO cells (5000/well) into 96-well plates for cAMP quantification. For stimulation curves (EC_{50} determinations), CHO-hV2R cells were stimulated by increasing AVP concentrations in the absence (control conditions) or in the presence of increasing competitor concentrations in a total 50 µl volume incubation medium containing DMEM, 5% BSA and 0.1 mM RO201724. For competition curves, 1.77 nM AVP stimulated CHO-hV2R cells in the absence (control conditions) or presence of increasing competitor concentrations. Experiments lasted for 30 min at 37 °C and were stopped by the addition of 25 µl of lysis buffer from the cAMP Dynamic 2 kit (Cisbio-International) containing cAMP labeled with acceptor entity first then by the addition of 25 µl of lysis buffer containing donor fluorophore-labeled antibody against cAMP (100 µl total volume per well). The fluorophores elicited a FRET signal (F% = 100 x (Rpos - Rneg)/Rneg) with Rpos fluorescence ratio (665/620 nm) measured in wells incubated with both donor- and acceptor-labeled entities, and Rneg being the same ratio for the negative control with donor fluorophore-labeled antibody only. This signal was then transformed into cAMP concentration in wells using a calibration curve. Activation/inhibition curves were plotted to the log of AVP concentrations and fitted to the Hill equation to extract the EC_{50}/IC_{50} using Graphpad Prism software. The corresponding Arunlakshana-Shild plots allowed to determine pA2 from the Schild equation. Experiments were done in triplicate. Data are presented as mean ± SEM.

2.4 *In vivo* experiments . The CEA animal experiment ethic committee approved the use of animals and experimental protocols (reference: APAFIS#1496-2015082111349702 v1). Six-week-old male Sprague-Dawley rats were obtained from Janvier Labs (Le Genest Saint Isle, France) and hosted in CEA Saclay animal facilities under stable and controlled conditions of temperature and pressure. They had free access to the standard rodent diet and tap water. Metabolic cages were purchased from Tecniplast (Buguggiate, Italie). After 3 days in metabolic cages for habituation, rats were intraperitoneally injected with 0.5 ml/kg of the toxin or vehicle dissolved in 0.9% NaCl solution. Urine outputs were collected 24 hours post-injection and weighed. Animal weight, food and water intakes were also measured for control. Urinary pH was measured using a pH-meter SevenEasy (Mettler Toledo, Viroflay, France). Urinary osmolality was measured using a Type 13 automatic osmometer (Roebling, Berlin, Germany). Urinary flow (UF) and Osmole excretion were reported to animal weight to avoid bias. UF = urinary volume/(time x body weight). Osmole excretion = (urinary osmolality x urinary volume)/(time x body weight).

2.5 Peptide production . All the peptides were synthesized on a Prelude synthesizer (Protein Technologies(r), Tucson, USA), purified and folded according to the method already described (Ciolek et al., 2017). Briefly, the solid-phase synthesis using a Fmoc strategy was done on 25 µmol of ChemMatrix®, peptide

cleavage and purification. Linear peptides were folded in the presence of oxidized and reduced glutathione (1 mM) and glycerol 20% (K10A) or guanidine 0.5 M (MQ2) in Tris buffer at pH 8 overnight at room temperature. All the other peptides were folded in presence of oxidized and reduced cysteine (1 and 0.1 mM, respectively), in Hepes 100 mM at pH 7.5 (R44A, MQ4, MQ5, MQ6, B4ESA3, C1IC51, D5J9Q8, F8J2F6 and Q5ZPJ7) and acetonitrile 20% (F18A, E7FL11 and P19859) or guanidine 0.5 M (MQ3, N-ter, N&C-ter, N6E, F21A, S24G, Q25A, K26A, K26E, K29A, H31F, V9S, N15A, F18A, S19A, T34F, K39A, K39E, K39W, N41A, S46R) or in Tris at pH 7.2 and guanidine 0.5 M (F17A and K10E), overnight at room temperature.

2.6 Phylogenetic reconstruction. We used mafft v7.388 -auto option 4 to align eight MQ with 40 dendrotoxin full mature sequences from VenomZone (https://venomzone.expasy.org/) and three bovine protease inhibitors with the Kunitz fold included as outgroup (UniProt IDs: P00974, P00975, and P04815). With this multi-sequence alignment, we obtained a Maximum Likelihood (ML) tree with RAxML version 8.2.7 5 under the PROTGAMMAJTT substitution model and the rapid hill climbing option (-f d). We calculate 15,000,000 trees with MrBayes v3.2.6 6 in three independent runs with four chains each under the JTT substitution model and rates = invgamma. We merged the 1,000 trees with best posteriors from each run and annotated the branches of the ML tree with RAxML -b option.

2.7 Statistical analysis. All statistical tests were performed with Kaleidagraph (Synergy software, Reading, USA). Multiple group comparisons were performed using a one-way ANOVA with post hoc test according to Dunnett. $P < 0.05$ was considered statistically significant. Values are expressed as means ± SEM.

3- RESULTS

3.1 Mamba venoms, a source of V2R inhibitory toxins

Mambas (genus *Dendroaspis*) are venomous African Elapidae snakes, whose bites are often deadly without proper medical treatment. They live throughout sub-Saharan Africa in savannas and in tropical rain forest (Ainsworth et al., 2017). MQ1 was discovered in the *Dendroaspis angusticeps* (Da) venom by function-based screening (Ciolek et al., 2017). The same strategy was applied to three other mamba venoms (Fig. 2). One gram of each *Dendroaspis polylepis* (Dp),*Dendroaspis jamesoni* (Dj) and *Dendroaspis viridis* (Dv) venoms were firstly fractionated by strong cation exchange liquid chromatography (Fig. 2A-C). Seven fractions (DpS, DpL, DjkN, DvC, DvG, DvK, DvL) inhibited tritiated vasopressin (^{3}H-AVP) binding on the human V2R stably expressed in a CHO cell line. These fractions were submitted to reverse phase liquid chromatography (Supplementary Fig. 1) to isolate DvGB (MQ2), DpSH (MQ3), DvKN (MQ4), DjkNE (MQ5), DvLM (MQ6) and DvCK (MQ9) containing one toxin each fully sequenced by mass fragmentation strategies (Supplementary Fig. 2). The DpLK fraction contains two peptides, one previously described as DTX-B (Strydom and Joubert, 1981), that we refer to as MQ7, and a novel homologue with the A27S substitution (MQ8). The list of the active fractions, their masses and number of disulfide bridges, as well as their proportions in the venom are summarized in Supplementary Table 1. Synthetic analogues of MQ2 to MQ6 were produced by solid phase chemical synthesis (Supplementary Fig. 3). We succeeded in the synthesis of the linear forms of the three MQ7, MQ8 and MQ9, but failed in their oxidation steps. Consequently, their pharmacological characterizations were limited by the availability of natural products found in the venoms. In addition, MQ7 and MQ8 could not be separated from each other, thus we characterized the effects of the MQ7/8 mix (DpLK fraction).

Binding competition experiments on hV2R showed that these novel MQs inhibit ^{3}H-AVP binding with affinities in the 1-100 nM range (Fig. 2D, Table 1). Moreover, MQs dose-dependently inhibited AVP-induced cAMP production measured on a CHO cell line stably expressing hV2R (Fig. 2E, Table 1), highlighting their antagonist activity (MQs never induced a cAMP production by themselves). The*in vivo* diuretic effects of the synthetic MQs (MQ1-MQ6) were investigated in Sprague-Dawley male rats after a single i.p. injection. Control rats urinated an average of 43 ml/day/kg BW. MQ1-5 (30 nmol/kg BW) increased diuresis by 6.5-fold without any loss of electrolytes (Table 2). MQ6, displaying a lower affinity for V2R and a lower potency to inhibit cAMP production *in vitro* was tested at 100 and 300 nmol/kg BW, and a 2-fold increase in diuresis at the highest dose was observed. Irrespective of the MQ tested or the dose used, urine osmolality variation

is inversely proportional to aquaresis modification (Table 2), demonstrating a pure aquaretic effect of the MQs.

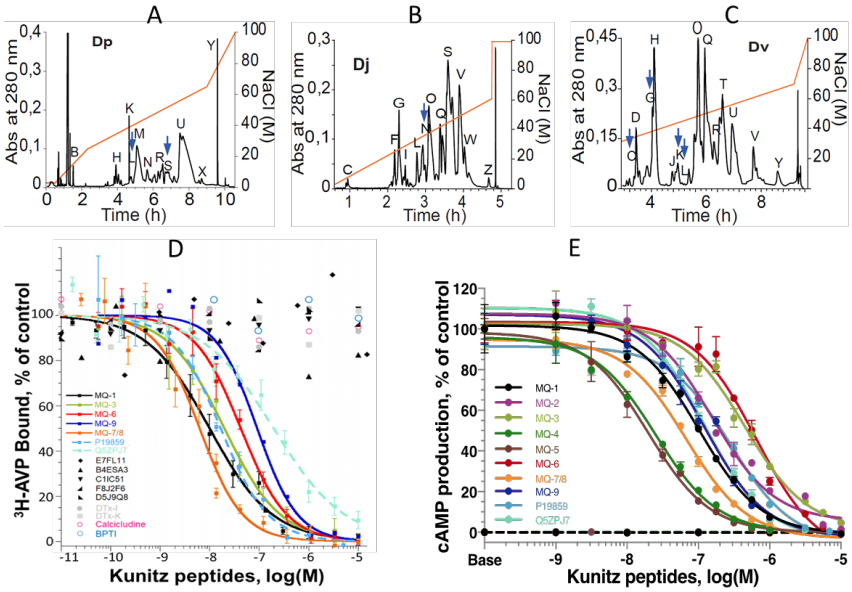

Figure 2: Identification and characterization of the MQs. Strong cationic exchange chromatography of Dp **(A)** , Dj**(B)** and Dv **(C)** . Blue arrows indicate active fractions on hV2R able to inhibit more than 50% of ^{3}H-AVP binding. **(D)** Binding of ^{3}H-AVP on hV2R in the presence of MQs (colored squares, for a comparison of the complete set of toxins, see Supplementary Table 2), P19859 and Q5ZPJ7 (blue dashed lines), Dtx-I (grey dots), Dtx-K (grey squares), calcicludine (pink open circle), BPTI (light blue open circle) or five other non-active Kunitz peptides (black symbols). α-DTX, MQ2, MQ4 and MQ5 curves are not shown for clarity. **(E)** Toxin antagonist effect on cAMP production induced by 1.77 nM of AVP on V2R (same color code than for panel D). Dotted line corresponds to cAMP production with toxins in the absence of AVP.

Table 1: Pharmacological properties of the V2R toxins. ND: not done. The statistical significance was assessed for binding by a one-way ANOVA with post hoc test according to Dunnett in comparison to MQ1. *: p value=]0.0; 0.01]; **: p value=]0.01; 0.001]; ***: p value < 0.001 and for cAMP inhibition by t-student in comparison to MQ1 with ***: p value < 0.001. Means represent 2 to 25 independent experiments. MQ7-8: MQ7 + MQ8. Calci: calcicludine

	Binding	Binding	Binding	Binding	Binding	Binding	AVP-induced cAMP inhibition	AVP-induced cAMP inhibition	AVP-induced cAMP inhibition	AVP-induced cAMP inhibition	AVP-induced cAMP inhibition	A i c
	K_i nM	K_i nM	Ratio K_i	pK_i	SEM	n	K_i nM	K_i nM	Ratio K_i	pK_i	SEM	n
MQ1	5.02		-	8.44	0.1	25	41		1	7,42	0,05	1
MQ2	8.16		1.6	8.17	0.15	4	98		2.4	7,04	0,1	3
MQ3	13.3		2.6	7.92	0.14	4	198	***	4.8	6,71	0,07	3
MQ4	7.34		1.5	8.27	0.21	5	12		0.3	7,97	0,1	3
MQ5	3.50		0.7	8.58	0.3	4	9		0.2	8,17	0,3	5
MQ6	21.5	*	4.3	7.60	0.1	5	251	***	6.1	6,66	0,2	3

	Binding	Binding	Binding	Binding	Binding	Binding	AVP-induced cAMP inhibition	AVP-induced cAMP inhibition	AVP-induced cAMP inhibition	AVP-induced cAMP inhibition	AVP-induced cAMP inhibition	A i c
MQ7-8	3.14		0.6	8.53	ND	2	25		0.6	7,65	0,2	3
MQ9	45.1	**	9.0	7.35	ND	2	48		1.2	7,35	0,1	3
P19859	7.87		1.6	7.93	0.08	4	91		2.2	7,07	0,1	3
Q5ZPJ7	112 ***	112 ***	22.2	6.97	0.08	4	61		1.5	7,27	0,1	3
E7FL11	>>1000	>>1000		<<5		2	ND	ND				
B4ESA3	>>1000	>>1000		<<5		2	ND	ND				
C1IC51	>>1000	>>1000		<<5		2	ND	ND				
D5J9Q8	>>1000	>>1000		<<5		2	ND	ND				
F8J2F6	>>1000	>>1000		<<5		2	ND	ND				
D-DTx	>>1000	>>1000		<<5		2	ND	ND				
DTx-K	>>1000	>>1000		<<5		2	ND	ND				
α-DTx	>>1000	>>1000		<<5		2	ND	ND				
DTx-I	>>1000	>>1000		<<5		2	ND	ND				
Calci	>>1000	>>1000		<<5		2	ND	ND				
BPTI	>>1000	>>1000		<<5		2	ND	ND				

Table 2: *In vivo* properties of V2R toxins. Statistical test was assessed by a one-way ANOVA with post hoc test according to Dunnett in comparison to control. *: p value=]0.05; 0.01]. **: p value=]0.01; 0.001]. ***: p value < 0.001. BW: body weight.

	n	Dose (nmol /kg BW)	24h diuresis (ml/kg)	24h diuresis (ml/kg)	SEM	Osmolality (mOsm /kg H2O)	Osmolality (mOsm /kg H2O)	SEM	Osmoles excretion (µOsmol/h /kg BW)
Control	6		43		4	1279		200	2137
MQ1	9	30	283	***	20	227	***	10	2728
MQ2	6	30	235	***	20	326	***	70	2940
MQ3	6	30	196	**	20	289	***	30	2277
MQ4	5	30	369	***	50	209	***	40	2826
MQ5	6	30	264	***	40	240	***	20	2592
MQ6	3	300	81	*	20	765	*	100	2360
P19859	3	100	69	*	10	779	*	30	2215
Q5ZPJ7	3	30	94	*	10	726	*	75	2712

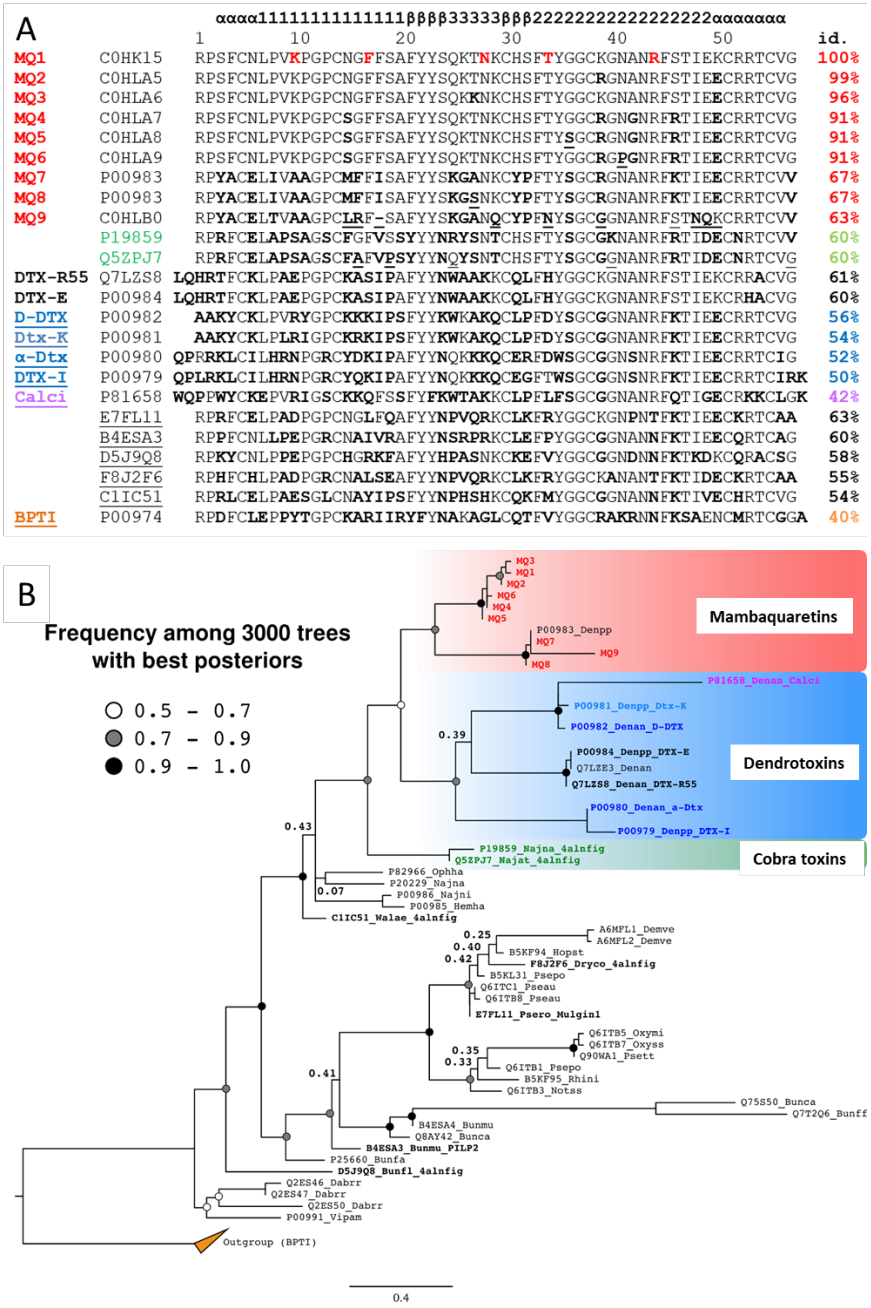

Figure 3: Amino acid sequences and phylogenetic organization of Kunitz toxins. **(A)** Sequence alignment according to the MQ1 sequence. Greek letters indicate MQ1 secondary structures, α for alpha helix, β for beta strain. Arabic numbers design MQ1 loops, loop 1 from residue 7 to 20, loop 2 from residue 32 to 49, loop 3 from residue 25 to 29. Red: toxins from Mamba active on V2R. Green: toxins from cobra active on V2R. Blue: toxins from Mamba active on Kv1.1. Pink: toxins from Mamba active on Cav. Orange: BPTI. Black: Unknown activities. Underline names: peptides not active on V2R. Bold residues are different from MQ1. MQ1 red residues are specific for V2R Kunitz-type peptides. Calci: calcicludine P81658. BPTI: Bovine Pancreatic Trypsin Inhibitor. Id: percentage of sequence identity to MQ1. **(B)** Maximum likelihood (ML) tree of MQ proteins and related sequences obtained with RAxML. Branches with at least three sequences

were annotated with the average frequency of ML tree bipartition among the 3000 trees with best posterior probabilities for each one of three chains of a MrBayes 3.2.6 run (top 1000 per run). Average bipartition frequency: 0.5-0.7, white circles; 0.7-0.9 grey circles; 0.9-1.0 black circles. Sequences in the alignment of panel A are highlighted in bold characters. Scale bar represents substitutions per site. Protein identifiers follow the same color scheme as panel A.

3.2 Mambaquaretins form a distinct group of Kunitz-type snake toxins

Amino acid sequences of Kunitz peptides were aligned according to MQ1 with representative sequences of dendrotoxins and three BPTI sequences (P00974, P00975 and P04815, Fig. 3A). This alignment was used to reconstruct the phylogenetic relationships of Kunitz-type snake toxins. The phylogram showed that all nine MQs constitute a well-supported monophyletic group, sister to ion-channel modulators isolated from mambas (so-called dendrotoxins). MQs are organized into two sub-groups: MQ1 to MQ6 are very closely-related to each other, whereas MQ7 to MQ9 are more divergent (Fig. 3B, red background). MQ8 is a natural variant of the dendro-B (P00983, named here MQ7), a weak trypsin inhibitor (Strydom and Joubert, 1981). Both diverge from MQ1 by 19 mutations. MQ9 is the most original sequence with 21 mutations compared to MQ1 and a one residue shorter loop 1 (Fig. 3A). All MQs are a sister group to a branch composed of seven dendrotoxins (Fig. 3B, blue background). The peptides DTX-R55 (Q7LZS8) and DTX-E (P00984) have never been characterized and are probably active on serine proteases as they possess the dyad Lys15-Ala16. The five other dendrotoxins are potassium and calcium channel inhibitors, which are not active on V2R up to 10 μM (Fig. 2D).

The next group is composed of two cobra toxins (Fig. 3B, green background). P19859 is an uncharacterized toxin from the Indian cobra Naja naja (Shafqat et al., 1990). Q5ZPJ7 is a weak chymotrypsin inhibitor from the Chinese cobra Naja atra (Zhou et al., 2004). The synthetic versions of P19859 and Q5ZPJ7 (Supplementary Fig. 4) bind V2R (Fig. 2D) and antagonize cAMP production (Fig. 2E, Table 1) with K_i and K_{inact} equivalent to those of other MQs. Injected in rats, both cobra toxins raise diuresis (2-fold increase) with a concomitant decrease of urine osmolality, demonstrating an aquaretic effect (Table 2). The other sequences used to build the phylogram belong for the most part to viper or Australian snakes. Among them, we checked the activity of five selected toxins (E7FL11, B4ESA3, D5J9Q8, F8J2F6 and C1IC51, Supplementary Fig. 4) distributed all along the dendrogram and having a dyad composition compatible with V2R activity (Asn15-Gly16, Asn15-Ala16 or His15-Gly16). None of them were active on V2R up to 10 μM (Fig. 1D).

The nine MQs constitute a new phylogenic Kunitz group associated with a V2R activity. The comparison between the 11 V2R-active toxin sequences and the non-active V2R Kunitz peptides highlighted 5 positions that might play positive roles in binding to the V2R (Fig. 3A, supplementary Fig. 5). The positions 17, 28, and 44 are strictly conserved in V2R-active Kunitz and highly variable in non-active V2R Kunitz. The position 34 is occupied by a threonine residue for 10 toxins and by an asparagine for one. It is highly variable in non-active V2R Kunitz. Finally, the position 10 is basic (Lys) or neutral (Ala, Ser) in V2R-active Kunitz whereas it is mostly acidic in other Kunitz groups (Fig. 3A, supplementary Fig. 5).

3.3 MQ1 uses its two large loops to bind V2R

To characterize the importance of the 5 positions described above for hV2R interaction, we synthesized the variants K10E, F17A, N28A, T34A, and R44E. We couldn't obtain the folded N28A variant. The 5 remaining variants induced a loss of 20 to 1340 fold in binding affinity (Fig. 4 and supplementary Table 2). Interestingly, they all belong to the MQ1 loop 1 and 2 (Fig. 3A). We expanded our analysis to other neighboring positions excluding structural (Cys, Ala, Gly, Pro) and buried positions (Tyr22, Tyr23, Phe33, Tyr35). We found that residues Val9 and Phe18 but not Ser19, Asn41 or Ser46 are in interaction with the V2R. Surprisingly, while the variants K39E and K39W never modified MQ1 affinity on hV2R, the K39A improved it by almost 9 times (Fig. 4, Supplementary table 2). We confirmed here previously demonstrated data showing that the N and C-terminal extremities (Fig. 4) are not involved in the binding process of MQ1 (Ciolek et al., 2017). Finally, the structured part of the toxin defined by residues implied in α-helix

or β-sheets, never participate to V2R binding as the variants N6E, F21A, S24G, Q25A, K26A, K26E, K29A and H31F displayed the same affinities for hV2R as MQ1.

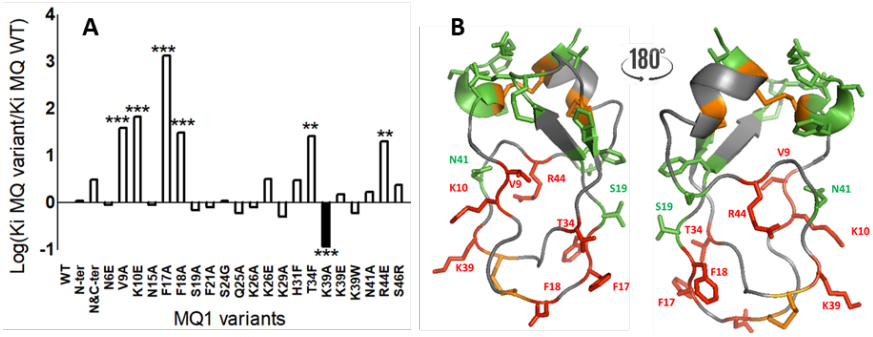

Figure 4: Structure-activity relationships of MQ1. **(A)**Affinities ratios of MQ1 variants. **: p value=]0.01; 0.001]. ***: p value < 0.001. N-ter: MQ1 without the four first residues RPSF. N&C-ter: MQ1 without the four first residues RPSF without the two last residues GV and with the terminal cysteine residue being amidated. **(B)** Front and back sticky representation of tested MQ1 positions (PDB: 5m4v). Variants which influence (red) or not (green) on MQ1 affinity for hV2R are shown.

3.4 MQ1-K39A is specific for human V2R.

We deepen the study of the variant MQ1-K39A as the substitution of a lysine residue by an alanine one significantly improves MQ1 affinity for hV2R. MQ1 and MQ1-K39A shifted to the right the AVP-dependent cAMP production on CHO cell lines expressing the hV2R (Fig. 5A-B). Arunlakshana–Schild plots show a purely competitive behavior between vasopressin and the toxins as IC_{50} regression can be linearized with slope close to unit (0.84 ± 0.04 for MQ1 and 0.99 ± 0.06 for MQ1-K39A, Fig. 5C). MQ1-K39A is 5.4 times more potent than MQ1 with a pA2 of 8.28 ± 0.08 (K_{inact} of 5.6 ± 0.9 nM) compared to a pA2 of 7.6 ± 0.2 for MQ1 (K_{inact} of 30 ± 7 nM). When 3 nmol/kg BW of toxins were injected in rats (i.p. route), 24h diuresis increased from 1.8 ml/kg/h (controls) to 5.0 ml/kg/h for MQ1 or 5.5 ml/kg/h for MQ1-K39A. Unexpectedly, MQ1-K39A did not induce stronger diuresis. In addition, this variant showed equivalent pharmacodynamics compared to MQ1 (Fig. 5E). To explain this discrepancy between human and rat V2R, we measured the affinity of MQ1 and MQ1-K39A for rat V2R. As published, MQ1 displays the same affinity for both species (K_i of 5.3 and 6.13 nM for human and rat V2R, Droctové et al., 2020). On its side, MQ1-K39A displayed similar affinity for rat V2R (K_i = 7.73 nM, pK_i = 8.37 ± 0.74, Fig. 5F) than MQ1 for hV2R (K_i = 4.7 nM), explaining why MQ1-K39A never induced higher diuresis on rat than MQ1.

Hosted file

`image5.emf` available at https://authorea.com/users/423476/articles/528864-a-new-kunitz-type-snake-toxin-family-associated-with-an-original-mode-of-interaction-with-the-vasopressin-2-receptor

Figure 5: *In vitro* and *in vivo* characterization of MQ1-K39A. Competitive inhibition of AVP-induced cAMP production in stable CHO-hV2R of MQ1 **(A)** and MQ1-K39A **(B)** .**(C)** Corresponding Arunlakshana–Schild plots. Schild representations are plotted as mean ± SEM, n = 4 (MQ1, red) or 5 (MQ1-K39A, blue). **(D)** Cumulated 24 h rat diuresis after administration by i.p. route. Black: Vehicle. Red: 3 nmol/kg BW of MQ1, Blue: 3 nmol/kg BW of MQ1-K39A, n = 6. **(E)** Rat diuresis versus time post-injection at 3 nmol/kg BW. Same color code. **(F)**Representative binding competition curves of MQ1 (red) and MQ1-K39A (blue) on hV2R (full line) and rV2R (dashed line, n = 3), expressed as mean ± SEM.

4- DISCUSSION

In this work, we enlarge the Kunitz-type toxin family active on the V2 vasopressin receptor through identification and characterization of novel mamba and cobra V2R antagonist ligands. Thanks to screening experiments and phylogenetic analysis, these structured ligands enable us to understand a new molecular mechanism for their interaction with the V2R.

Mamba (African) and cobra (here Asian species) are two evolutionary- and geographically-distant snakes. The presence of a cobra toxin group also active on V2R suggests either 1) independently derived V2R-activity of Kunitz toxins from cobras and mambas, or 2) conserved V2R-activity due to shared ancestry (ion-channel blockade of dendrotoxins would be the derived activity then). The presence of toxins active on V2R in various Elapid snake venoms suggests an important role of these toxins for snakes' survival. However, whether or not the V2R activity is their selected function in the ecological context of venom use remains to be established. We note that as long as victim has access to water, blockage of V2R shouldn't be toxic at all. In any case, the screening of new targets, like GPCRs, allowed us the discovery of new group of toxins with a strong activity on a pharmaceutically relevant receptor, highlighting the extraordinary diversity of animal toxins present in venoms that remains largely underexplored.

The identification of a new monophylogenic group in the Kunitz peptide family constituted a great opportunity to better understand the molecular mechanisms supporting the pharmacological property of these toxins. The natural SAR highlighted the importance of the 2 MQ1 major loops in V2R binding, which was confirmed by an extended number of characterized MQ1 variants. MQ1 shows a new strategy to bind to its target compared to α-DTX (Fig. 1, Gasparini et al., 1998) and BPTI (Fig. 1, Kawamura et al., 2011). Indeed, whereas α-DTX uses its structured part to block Kv1.1 and BPTI its loop 1 to inhibit serine-proteases, MQ1 exploited its 2 major loops and engages more positions in its interaction with V2R. The pharmacophore defined by numerus amino acids positioned in loop 1 (9 to 18) and loop 2 (34, 39 and 44) may be at the origin of the absolute selectivity of MQ1 for the V2R.

MQ1 displays the same nanomolar affinity for rat and human V2R (Droctové et al., 2020) but no interaction with V1aR, V1bR or OTR (Ciolek et al., 2017). The figure 6 shows a sequence alignment between the 3 external loops (ELs) of the vasopressin-sensitive receptors. When comparing these 5 receptor sequences, 9 positions appeared as V2R specific *versus* V1Rs and OTR. Three are acidic residues: D103 (numbering according to the hV2R) in ECL1, E198 in ECL2, E299 in ECL3 and 6 are non-polar residues, all in ECL3. The 3 MQ1 basic residues implied in V2R binding (K10, K39, R44) and the 3 V2R specific acidic residues just described, point to a charge complementarity between the two partners. In addition to these 9 specific positions, differences in loop length may play a role in the MQ1 selectivity. OTR ECL2 is shorter by 2 residues compared to V2R while the V1Rs ECL3 ones are longer by 3 residues. Even if extensive structure-activity-relationships should be done to validate these hypotheses, these data describe the implication of important residues covering a large surface of contact for MQ1, which appear to be in coherence with a possible implication of the 3 V2R ECLs in the complex MQ1/V2R formation.

MQ1-K39A showed an interesting 14-fold higher specificity for hV2R*versus* rV2R. Too many mutations exist between rat and human V2R sequences to propose any hypothesis but MQ1-K39A represent a new tool to gain insights into its mode of action. Blocking the V2R is a validated therapeutic line for several pathologies like the autosomal dominant polycystic kidney disease (Juul et al., 2014). Improving the *in vivo* activity of MQ1 is important to develop a new therapeutic option for V2R-related diseases. This work presents an upgraded version of MQ1, which can not be validated on rats, showing the limits of rat animal model.

	ECL1	ECL2	ECL3
	103	198	292 299 306 310
hV2R	WKAT**D**RFRGPD	QRNVEGGSGVTDCWACFA**E**PWGRRT	VQ**L**W**A**AWDP**E**AP**L**-EGA**P**F**V**--L**L**MLL
rV2R	WDAT**D**RFHGPD	QRDVGNGSGVFDCWARFA**E**PWGLRA	VQ**L**W**A**AWDP**E**AP**L**-EER**P**P**V**--L**L**MLL
hV1aR	WDITYRFRGPD	MIEVNNVTKARDCWATFIQPWGSRA	IQMWSVWDPMSVWTESENPTITITALL
hV1bR	WDITYRFRGPD	LREVIQGSGVLDCWADFGFPWGPRA	VQMWSVWDKNAPDEDSTNVAFTISMLL
hOT	WDITFRFRGPD	LREVAD--GVFDCWAVFIQPWGPKA	VQMWSVWDANAPK-EASAFI--IVMLL

Figure 6 : Sequence analysis of vasopressin-sensitive receptors. In bold, residues which are identical between

rat (r) and human (h) V2Rs but variable in hV1aR, hV1bR or hOT. Red: acidic residues. Orange: non-polar residues. ECL: extracellular loop.

The Kunitz structure is active on 3 major classes of molecular targets: enzymes, channels and receptors. It is a rare situation in animal toxins where each structure is linked in great part to only one activity. Only the 3FT family, exclusively produced by snakes, target also these 3 classes of proteins that are enzymes (serine proteases for BPTI, acetylcholine esterase for fasciculins, Bourne et al., 1995), ion channels (Kv1.1 for the dendrotoxins, ASIC channel for the mambalgins, Sun et al., 2018) and GPCRs (V2R for MQ1, Muscarinic and adrenergic receptors for aminergic toxins, Quinton et al., 2010; Rouget et al., 2010; Blanchet et al., 2017). The 3FT toxins are composed of 3 loops called fingers linked by a structured part rich in disulfide bridges (Fruchart-Gaillard et al., 2012). 3FTs always use their fingers to interact with their targets. The fasciculins and the mambalgins use their first and second fingers while the MT7 uses all of its 3 fingers (Maeda et al., 2020). The Kunitz peptides show much more adaptive binding strategies. For each target class, a distinct mode of action is used by these peptides. The mode of interaction of MQ1 to bind V2R is particularly efficient as MQ1 is the most selective V2R ligand ever described.

5- REFERENCES

Ainsworth, S., Petras, D., Engmark, M., Süssmuth, R.D., Whiteley, G., Albulescu, L., et al. (2017). The medical threat of mamba envenoming in sub-Saharan Africa revealed by genus-wide analysis of venom composition, toxicity and antivenomics profiling of available antivenoms. J. Proteomics.

Andreev, Y. a., Kozlov, S. a., Koshelev, S.G., Ivanova, E. a., Monastyrnaya, M.M., Kozlovskaya, E.P., et al. (2008). Analgesic compound from sea anemone Heteractis crispa is the first polypeptide inhibitor of vanilloid receptor 1 (TRPV1). J. Biol. Chem. *283* : 23914–21.

Blanchet, G., Alili, D., Protte, A., Upert, G., Gilles, N., Tepshi, L., et al. (2017). Ancestral protein resurrection and engineering opportunities of the mamba aminergic toxins. Sci. Rep. *7* : 2701.

Blanchet, G., Collet, G., Mourier, G., Gilles, N., Fruchart-Gaillard, C., Marcon, E., et al. (2014). Polypharmacology profiles and phylogenetic analysis of three-finger toxins from mamba venom: Case of aminergic toxins. Biochimie *103* : 109–117.

Bohlen, C.J., Chesler, A.T., Sharif-Naeini, R., Medzihradszky, K.F., Zhou, S., King, D., et al. (2011). A heteromeric Texas coral snake toxin targets acid-sensing ion channels to produce pain. Nature *479* : 410–4.

Bourne, Y., Taylor, P., and Marchot, P. (1995). Acetylcholinesterase inhibition by fasciculin: Crystal structure of the complex. Cell*83* : 503–512.

Ciolek, J., Reinfrank, H., Quinton, L., Viengchareun, S., Stura, E.A., Vera, L., et al. (2017). Green mamba peptide targets type-2 vasopressin receptor against polycystic kidney disease. Proc. Natl. Acad. Sci. U. S. A. *114* : 7154–7159.

Droctové, L., Lancien, M., Tran, V.L., Susset, M., Jego, B., Theodoro, F., et al. (2020). A snake toxin as a theranostic agent for the type 2 vasopressin receptor. Theranostics *10* : 11580–11594.

Fruchart-Gaillard, C., Mourier, G., Blanchet, G., Vera, L., Gilles, N., Ménez, R., et al. (2012). Engineering of three-finger fold toxins creates ligands with original pharmacological profiles for muscarinic and adrenergic receptors. PLoS One *7* : e39166.

Gasparini, S., Danse, J.M., Lecoq, A., Pinkasfeld, S., Zinn-Justin, S., Young, L.C., et al. (1998). Delineation of the functional site of α-dendrotoxin: The functional topographies of dendrotoxins are different but share a conserved core with those of other Kv1 potassium channel-blocking toxins. J. Biol. Chem. *273* : 25393–25403.

Harper, E., and Berger, A. (1967). On the size of the active site in proteases: I. Papain. Biochem. Biophys. Res. Commun. *27* : 157–162.

Harvey, A.L. (2001). Twenty years of dendrotoxins. Toxicon *39* : 15–26.

Huber, R., Kukla, D., Rühlmann, A., Epp, O., and Formanek, H. (1970). The basic trypsin inhibitor of bovine pancreas. I. Structure analysis and conformation of the polypeptide chain. Naturwissenschaften *57* : 389–92.

Juul, K.V., Bichet, D.G., Nielsen, S., and Nørgaard, J.P. (2014). The physiological and pathophysiological functions of renal and extrarenal vasopressin V2 receptors. Am. J. Physiol. Renal Physiol. *306* : F931-40.

Kawamura, K., Yamada, T., Kurihara, K., Tamada, T., Kuroki, R., Tanaka, I., et al. (2011). X-ray and neutron protein crystallographic analysis of the trypsin-BPTI complex. Acta Crystallogr. D. Biol. Crystallogr. *67* : 140–8.

Kessler, P., Marchot, P., Silva, M., and Servent, D. (2017). The three-finger toxin fold: a multifunctional structural scaffold able to modulate cholinergic functions. J. Neurochem. *142 Suppl* : 7–18.

Kunitz, M., and Northrop, J.H. (1936). Isolation From Beef Pancreas of Crystalline Trypsinogen, Trypsin, a Trypsin Inhibitor, and an Inhibitor-Trypsin Compound. J. Gen. Physiol. *19* : 991–1007.

Maeda, S., Xu, J., N Kadji, F.M., Clark, M.J., Zhao, J., Tsutsumi, N., et al. (2020). Structure and selectivity engineering of the M1 muscarinic receptor toxin complex. Science *369* : 161–167.

Maïga, A., Mourier, G., Quinton, L., Rouget, C., Gales, C., Denis, C., et al. (2012). G protein-coupled receptors, an unexploited animal toxin targets: Exploration of green mamba venom for novel drug candidates active against adrenoceptors. Toxicon *59* : 487–96.

Otlewski, J., Jaskólski, M., Buczek, O., Cierpicki, T., Czapińska, H., Krowarsch, D., et al. (2001). Structure-function relationship of serine protease-protein inhibitor interaction. Acta Biochim. Pol. *48* : 419–28.

Quinton, L., Girard, E., Maiga, A., Rekik, M., Lluel, P., Masuyer, G., et al. (2010). Isolation and pharmacological characterization of AdTx1, a natural peptide displaying specific insurmountable antagonism of the alpha1A-adrenoceptor. Br. J. Pharmacol. *159* : 316–25.

Rouget, C., Quinton, L., Maïga, A., Gales, C., Masuyer, G., Malosse, C., et al. (2010). Identification of a novel snake peptide toxin displaying high affinity and antagonist behaviour for the α2-adrenoceptors. Br. J. Pharmacol. *161* : 1361–74.

Schweitz, H., Heurteaux, C., Bois, P., Moinier, D., Romey, G., and Lazdunski, M. (1994). Calcicludine, a venom peptide of the Kunitz-type protease inhibitor family, is a potent blocker of high-threshold Ca2+ channels with a high affinity for L-type channels in cerebellar granule neurons. Proc. Natl. Acad. Sci. *91* : 878–882.

Shafqat, J., Zaidi, Z.H., and Jörnvall, H. (1990). Purification and characterization of a chymotrypsin Kunitz inhibitor type of polypeptide from the venom of cobra (Naja naja naja). FEBS Lett. *275* : 6–8.

Strydom, D.J., and Joubert, F.J. (1981). The amino acid sequence of a weak trypsin inhibitor B from Dendroaspis Polylepis polylepis (black mamba) venom. Hoppe. Seylers. Z. Physiol. Chem. *362* : 1377–84.

Sun, D., Yu, Y., Xue, X., Pan, M., Wen, M., Li, S., et al. (2018). Cryo-EM structure of the ASIC1a – mambalgin-1 complex reveals that the peptide toxin mambalgin-1 inhibits acid-sensing ion channels through an unusual allosteric effect. Cell Discov. 1–11.

Zhou, X.D., Jin, Y., Lu, Q.M., Li, D.S., Zhu, S.W., Wang, W.Y., et al. (2004). Purification, characterization and primary structure of a chymotrypsin inhibitor from Naja atra venom. Comp. Biochem. Physiol. - B Biochem. Mol. Biol. *137* : 219–224.